Random-Phase Solitons in Nonlinear Periodic Lattices

Buljan, Hrvoje; Cohen, O.; Fleischer, Jason W.; Schwartz, T.; Segev, M.; Musslimani, Z. H.; Efremidis, N. K.; Christodoulides, D. N.

Source / Izvornik: **Physical Review Letters, 2004, 92**

Journal article, Published version
Rad u časopisu, Objavljena verzija rada (izdavačev PDF)

https://doi.org/10.1103/PhysRevLett.92.223901

Permanent link / Trajna poveznica: https://urn.nsk.hr/urn:nbn:hr:217:302687

Rights / Prava: In copyright / Zaštićeno autorskim pravom.

Download date / Datum preuzimanja: **2024-03-28**

Repository / Repozitorij:

Repository of the Faculty of Science - University of Zagreb

Random-Phase Solitons in Nonlinear Periodic Lattices

H. Buljan,[1,2] O. Cohen,[1] J.W. Fleischer,[1] T. Schwartz,[1] and M. Segev[1]
[1]*Physics Department, Technion–Israel Institute of Technology, Haifa 32000, Israel*
[2]*Department of Physics, University of Zagreb, PP 332, 10000 Zagreb, Croatia*

Z. H. Musslimani,[3] N. K. Efremidis,[3] and D. N. Christodoulides[3]
[3]*University of Central Florida, Orlando, Florida 32816, USA*
(Received 9 November 2003; published 3 June 2004)

We predict the existence of random phase solitons in nonlinear periodic lattices. These solitons exist when the nonlinear response time is much longer than the characteristic time of random phase fluctuations. The intensity profiles, power spectra, and statistical (coherence) properties of these stationary waves conform to the periodicity of the lattice. The general phenomenon of such solitons is analyzed in the context of nonlinear photonic lattices.

DOI: 10.1103/PhysRevLett.92.223901 PACS numbers: 42.65.Tg

Nonlinear systems with inherent periodicity are abundant in nature. Examples may be found in biology [1], chemical physics [2], nonlinear optics [3], Josephson-junction ladders [4], Bose-Einstein condensates (BEC) [5], etc. Optics especially has provided important advances and holds great promise for applications. Recent results in nonlinear waveguide arrays include the observation of discrete solitons [6], diffraction management [7], Bloch oscillations [8], the use of the optical induction technique to create nonlinear photonic lattices [9–11], the observation of spatial gap (staggered) solitons [10,11], higher band Floquet-Bloch (FB) solitons [12], the prediction of multiband vector lattice solitons [13], etc. (for a recent review, see Ref. [14]). Theoretically, nonlinear waveguide arrays have been mostly treated with the coupled mode theory, where dynamics is well approximated with the discrete nonlinear Schrödinger equation (NLSE) [3]. In a more general approach, the FB theory is used to analyze a continuous differential equation with a periodic potential term (e.g., the NLSE/Gross-Pitaevskii equation in the context of nonlinear optics/BEC). The main feature of wave propagation in periodic systems is the interference of waves reflected from the lattice, which drives the propagation dynamics. These interference effects depend crucially on the coherence of the waves. However, in nonlinear periodic lattices, only coherent waves have been considered thus far. Since most waves encountered in nature are only partially coherent, theories assuming perfectly coherent waves are idealizations, which are nevertheless accurate when the characteristic length describing the coherence of waves greatly exceeds the characteristic dimension of the system (e.g., the lattice spacing). However, when the two length scales are comparable, the interference effects, and consequently the dynamics, will depend on the interplay between the statistical (coherence) properties of the waves and the lattice periodicity. *Here we consider the propagation of partially coherent waves in nonlinear periodic lattices.*

The propagation of partially coherent light waves in homogeneous noninstantaneous nonlinear media was studied extensively in recent years [15–20]. It has been shown that the statistical properties of light greatly influence the dynamics (e.g., the properties of incoherent solitons [15–18,20] and modulation instability [19]).

In this Letter, we predict the existence of random phase solitons (RPS) in nonlinear periodic lattices. These solitons are found in media where the nonlinear response time is much longer than the characteristic time of random phase fluctuations. An RPS forms when the time-averaged intensity of an incoherent wave packet induces a defect in the periodic potential which has multiple bound states; the wave packet "binds" itself to that defect by randomly populating these states in a self-consistent fashion (on the time average). For RPSs to exist, their intensity profiles, power spectra and coherence properties must conform to the lattice periodicity.

The problem of partially coherent wave propagation in nonlinear periodic systems is general. However, for concreteness we analyze RPSs in the context of optics and use the corresponding terminology. The description of the physical system is as follows. A quasimonochromatic yet partially spatially incoherent cw beam is incident upon a noninstantaneous nonlinear medium (e.g., photorefractives, liquid crystals, etc.) with periodically modulated index of refraction. The characteristic time scales involved are the response time of the medium τ_m, the characteristic time of random fluctuations (the coherence time) τ_f, and the traveling time of light through the medium τ_t. When these time scales are related as $\tau_m \gg \tau_f \gg \tau_t$, the amplitude of the electric field $E(x, z, t)\exp(ikz - i\omega t)$ obeys (see Refs. [18,21] for derivation in homogeneous media):

$$i\frac{\partial E}{\partial z} + \frac{1}{2k}\frac{\partial^2 E}{\partial x^2} + \frac{V(x, z)k}{n_0}E = 0, \tag{1}$$

where the potential $V(x, z) = p(x) + \delta n(I)$ contains a

 © 2004 The American Physical Society

nonlinear $\delta n(I)$ and a periodic term $p(x) = p(x + D)$ with period D; the nonlinear index change δn depends on the time-averaged intensity I and is in temporal steady state, $\partial \delta n(I)/\partial t = \partial I/\partial t = 0$. Here $k = n_0\omega/c$, where n_0 is the linear part of the refractive index. The statistics describing random fluctuations of the electric field is expressed with the mutual coherence function $B(x_1, x_2, z) = \langle E(x_1, z, t)E^*(x_2, z, t)\rangle$ [18], where brackets $\langle \cdots \rangle$ denote the time average over τ_m. Instead of analyzing the evolution equation for the mutual coherence function [18], it is more convenient, but equivalent, to use the modal theory [17,21]. Within the modal theory, the field is expressed as a superposition of coherent waves with randomly varying coefficients: $E(x, z, t) = \sum_n c_n(t)\psi_n(x, z)$ [17]. The statistical properties of the light follow from $\langle c_n(t)c_{n'}^*(t)\rangle = d_n\delta_{nn'}$; that is,

$$B(x_1, x_2, z) = \sum_n d_n\psi_n(x_1, z)\psi_n^*(x_2, z), \tag{2}$$

while $I(x, z) = \sum_n d_n|\psi_n(x, z)|^2$. The functions $\psi_n(x, z)$ form an orthonormal set, and d_n denotes the power within the nth wave [21]. By inserting $E = \sum_n c_n\psi_n$ in Eq. (1), and using $\langle c_n c_{n'}^*\rangle = d_n\delta_{nn'}$, one finds the set of evolution equations for coherent waves ψ_n:

$$i\frac{\partial\psi_n}{\partial z} + \frac{1}{2k}\frac{\partial^2\psi_n}{\partial x^2} + \frac{V(x, z)k}{n_0}\psi_n(x, z) = 0, \tag{3}$$

where $V = p(x) + \delta n[\sum_n d_n|\psi_n(x, z)|^2]$.

Evolution Eq. (3) describes the dynamics of the system. In the absence of nonlinearity $[V(x) = p(x)]$, the eigenmodes of the system are FB waves, $\phi_\beta(x, z) = f_\beta(x)\exp[ik_x x + i\beta z]$, which are extended (not localized) states, organized into bands separated by gaps. Here, $f_\beta(x) = f_\beta(x + D)$ denotes the spatial profile of the FB wave. Its propagation constant β is a function of the Bloch wave vector k_x [see Figs. 1(a) and 1(b)]. When an incoherent beam enters such a linear system, each coherent wave ψ_n excites many FB waves ϕ_β, and the beam experiences diffraction in periodic medium [14]. In a nonlinear system, a stationary incoherent beam (RPS) can form if diffraction is exactly balanced by the nonlinearity. Stationary propagation occurs when the self-consistency loop is closed, i.e., when an incoherent beam consisting of randomly excited coherent waves ψ_n induces a defect in the lattice $\delta n[I(x)]$, which creates multiple localized (defect) states, some (or all) of which are *identical* to coherent waves ψ_n themselves. In this case, the propagation constants of the coherent waves (i.e., defect states) are in the gaps of the spectrum of the linear system, and it is convenient to expand the notation: $\psi_n \to \psi_{n,l} = u_{n,l}(x)\exp(i\kappa_{n,l}z)$. The propagation constant $\kappa_{n,l}$ of the coherent wave $\psi_{n,l}$ resides in the gap above the nth band [see circles in Figs. 1(a) and 1(b)], while l describes the hierarchy within a single gap: if $l < l'$ then $\kappa_{n,l} > \kappa_{n,l'}$. The spatial profiles $u_{n,l}(x)$ of the coherent waves obey

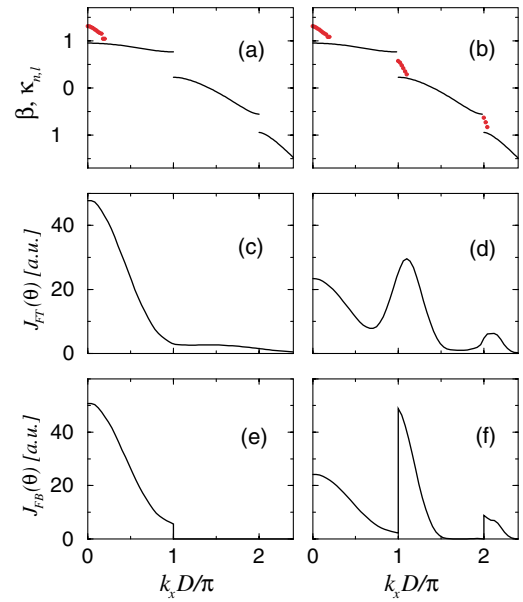

FIG. 1 (color online). The propagation constants and the power spectra of the RPSs. (a),(b) The diffraction curves $0.58kx_0^2\beta$ vs k_xD/π (solid curves) of the linear lattice, and the propagation constants $0.58kx_0^2\kappa_{n,l}$ (circles) of the (a) first band RPS and (b) three-band RPS. The Fourier power spectrum of the (c) first band RPS and (d) three-band RPS. The power spectra in the FB basis for the (e) first band soliton and (f) three-band soliton. The lattice is formed as $p(x) = p_0\sum_m e^{-[(x-mD)/x_0]^8}$, $p_0/n_0 \approx 1.74 \times 10^{-4}$, and $x_0/D = 0.37$.

$$\frac{1}{2k}\frac{d^2u_{n,l}}{dx^2} + \frac{\{p(x) + \delta n[I(x)]\}k}{n_0}u_{n,l} = \kappa_{n,l}u_{n,l}(x), \tag{4}$$

where $I(x) = \sum_{n,l} d_{n,l}|u_{n,l}(x)|^2$. The localized eigenmodes $\psi_{n,l}$ are randomly excited; their time-averaged occupancy is given by the modal weights $d_{n,l}$, while the time-averaged intensity $I(x) = \sum_{n,l} d_{n,l}|u_{n,l}(x)|^2$ induces the defect $\delta n[I(x)]$ which creates the localized eigenmodes $\psi_{n,l}$ themselves. The statistical properties of the solitons described above are stationary during propagation as $B(x_1, x_2) = \sum_{n,l} d_{n,l}u_{n,l}(x_1)u_{n,l}^*(x_2)$ is independent of z.

The statistical and diffraction properties of the RPS are intimately related to its spatial power spectrum [16], that we express in terms of the Fourier transform,

$$J_{\rm FT}(k_x) = \sum_{n,l} d_{n,l}\left|\int_{-\infty}^{\infty} dx u_{n,l}(x)e^{-ik_x x}\right|^2, \tag{5}$$

and by projecting the coherent waves onto the FB waves of the linear waveguide array,

$$J_{\rm FB}(k_x) = \sum_{n,l} d_{n,l}\left|\int_{-\infty}^{\infty} dx u_{n,l}(x)f_\beta^*(x)e^{-ik_x x}\right|^2. \tag{6}$$

The power spectra of RPS have generic features that follow from the qualitative analysis of diffraction in periodic media. Consider a wave packet exciting the FB waves around some transverse momentum value k_x. The

diffraction of such a wave packet depends on the curvature of the diffraction curve at k_x, $D_p(k_x) = \partial^2\beta(k_x)/\partial k_x^2$. In 1D periodic media, the diffraction coefficient $D_p(k_x)$ oscillates around zero, and the regions of normal $[D_p(k_x) < 0]$ and anomalous diffraction $[D_p(k_x) > 0]$ alternate. The nth Brillouin zone ($n = 1, 2, \ldots$) is split into the normal $[(n-1)\pi/D, \alpha_n)$, and anomalous diffraction interval $(\alpha_n, n\pi/D]$, where $D_p(\alpha_n) = 0$. If the beam is more incoherent, the width of its power spectrum is broader and may extend over a wide region in the k_x space [16], in which $D_p(k_x)$ significantly varies. As the self-focusing effect balances normal diffraction, we come to the following conclusion: If the nonlinearity is self-focusing, the power spectrum $J_{\mathrm{FB}}(k_x)$ of an RPS must be supported mainly in the (disjoint) normal diffraction intervals. The opposite occurs for the self-defocusing nonlinearity, where the power spectrum $J_{\mathrm{FB}}(k_x)$ covers mainly the anomalous diffraction intervals. This characteristic property of the FB power spectrum $J_{\mathrm{FB}}(k_x)$ is immediately reflected onto the Fourier power spectrum $J_{\mathrm{FT}}(k_x)$. Figures 1(c)–1(f) illustrate the power spectra of RPS (exact parameters are given below).

Up to this point, the analysis is general and applicable to different types of nonlinearities and periodic potentials. From now on we assume that the nonlinearity is self-focusing and saturable, $\delta n(I) = \gamma I/(1 + I/I_S)$, and the lattice is constructed in the form $p(x) = p_0\sum_m \exp-[(x - mD)/x_0]^8$ (m integer). The lattice sites (centers of the waveguide channels) are located at points $x = mD$, while the proximity of points $x = (m + 1/2)D$ corresponds to interstitial regions. The parameters used in the calculations are $n_0 = 2.3$, $p_0 = 4 \times 10^{-4}$, $x_0 = 3.7\ \mu$m, $D = 10\ \mu$m, and $k = n_0 2\pi/\lambda$, where $\lambda = 488$ nm, $\gamma I_S = 1.5 \times 10^{-4}$. We seek for RPS numerically and solve Eq. (4) with the iterative self-consistency method [17]. We restrict the analysis to symmetric solutions $I(x) = I(-x)$, where the mode profiles $u_{n,l}(x)$ are real functions constructed from waves with opposite transverse momenta $\pm k_{x,n,l}$, so that the total transverse momentum is zero. The power is distributed to the localized modes as $d_{n,l} \propto \exp[-l^2/(2w_n^2)]$ for $l \leq l_n$; l_n is the number of excited modes in the gap above the nth band. The characteristic features of RPS are illustrated in two examples, where the localized modes originate (i) solely from the first band [$l_1 = 11$, $w_1 = 4.34$, Figs. 2(a) and 2(b)], and (ii) from the first three bands [$l_1 = 11, l_2 = 6, l_3 = 3, w_1 = 4.34, w_2 = 2.36$, and $w_3 = 3.55$, Figs. 2(c)–2(f)]. The propagation constants $\kappa_{n,l}$ of the first and the three-band soliton are displayed as circles in Figs. 1(a) and 1(b), respectively. The total power within each soliton is $P = 94.3 I_S x_0$. For the three-band RPS, the amount of power within the modes from the first, the second, and the third band is 47%, 47%, and 6%, respectively. These solitons are stable in a wide parameter regime, as has been checked numerically by evolving them for many diffraction lengths with initial noise that contained 10% of the RPS power.

Let us analyze the common features and differences of the intensity, statistical, and diffraction properties of these RPS examples (see Fig. 2). In all cases, the envelope of the intensity profile encompasses several waveguide channels. Superimposed on this envelope there are oscillations in the intensity which conform to the lattice periodicity. From Fig. 2(a) we see that the intensity profile of the first band RPS has peaks that coincide with the lattice sites. In contrast, the three-band RPS has a large amount of power (~50%) in the interstitial regions [Fig. 2(c)]. We explain these differences by noting that the FB waves of the second and the third band contain a large amount of power in the interstitial regions, and from the fact that the localized modes originating from FB waves inherit their properties [13]. The intensity structure of the RPS induces a defect in the periodic potential, which is illustrated in Fig. 2(f) for the three-band RPS. The defect and the RPS are broad due to the fact that many localized modes are excited.

The coherence properties are described by (i) the complex coherence factor, $\mu(x, x') = B(x, x')/\sqrt{I(x)I(x')}$,

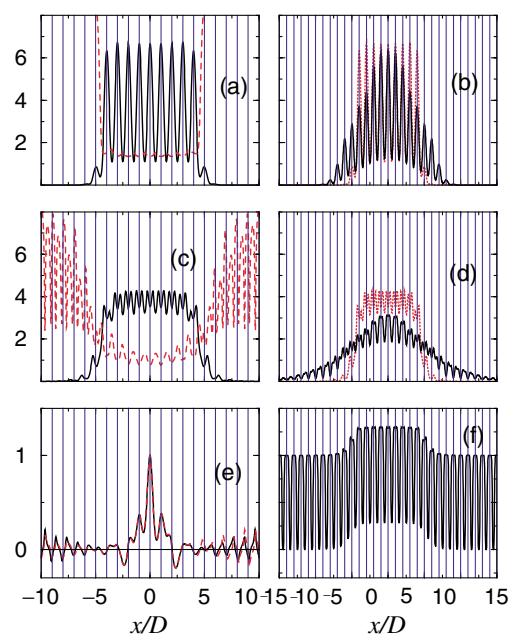

FIG. 2 (color online). The intensity profiles, diffraction, and spatial coherence properties of the RPSs. First band RPS: (a) the intensity profile $I(x)/I_S$ (solid line) and $l_s(x)/D$ (dashed line); (b) diffraction after 8.29 mm of propagation (solid line), and $I(x)/I_S$ at $z = 0$ (dashed line). Three band RPS: (c) $I(x)/I_S$ (solid line) and $l_s(x)/D$ (dashed line); (d) diffraction after 8.29 mm (solid line), and $I(x)/I_S$ at $z = 0$ (dashed line). (e) The complex coherence factors $\mu(x, 0)$ (solid line) and $\mu(x + D, D)$ (dashed line) of the three-band RPS. (f) The normalized induced potential $V(x)$ (defect) of the three-band RPS containing the periodic and nonlinear term. Vertical lines denote the lattice sites.

which expresses the degree of correlation between the field values at points x and x', and (ii) the spatial correlation distance $l_s(x) = \int_R dx' |\mu(x, x')|^2$, which gives the characteristic length scale describing spatial coherence; the region of integration R is several times larger than the soliton region. The common feature of the RPSs is that $l_s(x)$ exhibits oscillations that follow lattice periodicity and increases at the RPS tails [Figs. 2(a) and 2(c)]. The latter feature occurs because only the slowly decaying modal constituents are present at the tails, thereby increasing the spatial coherence. From Figs. 2(a) and 2(c) we observe that the spatial correlation distance $l_s(x)$ is approximately invariant under translations by D within the soliton region. The property $l_s(x) \approx l_s(x + D)$ is a consequence of an underlying approximate invariance law: $\mu(x, x') \approx \mu(x + D, x' + D)$. This is illustrated in Fig. 2(e) that shows $\mu(x, x')$, and $\mu(x + D, x' + D)$, for $x' \approx 0$; the graphs appear almost identical. We also observe that as $l_s(x)$ follows the lattice periodicity, it is lower at the lattice sites and increases in the interstitial regions. To explain this, consider modes originating from some band; the modes with smaller propagation constants extend further towards the RPS tails and also have more power in the interstitial regions. This increases $l_s(x)$ in the interstitial regions.

Diffraction of coherent waves in periodic media has been well studied [7,14]. Because diffraction is fundamentally a linear phenomenon, diffraction of an incoherent beam can be represented as a superposition of independently diffracting coherent waves $\psi_{n,l}$. The overall result depends on different weights $d_{n,l}$, transport directions, and diffraction coefficients associated to each coherent wave $\psi_{n,l}$. Figures 2(b) and 2(d) display the diffraction of the first and the three-band RPS after 8.29 mm of propagation (nonlinearity is off).

From the analysis above it follows that properties of an RPS are determined by the modal structure of the incoherent light. This is also valid for the power spectra. The Fourier power spectrum of the first band RPS [Fig. 1(c)] is single humped covering mainly the normal diffraction region of the first Brillouin zone, whereas the spectrum of the three-band soliton [Fig. 1(d)] is multihumped covering the normal diffraction regions of the first three Brillouin zones (for self-defocusing nonlinearity anomalous diffraction regions would be covered). The FB power spectra have similar properties, yet we numerically observe that the FB spectra of the localized modes originating from the nth band occupy *only* the nth Brillouin zone [Figs. 1(e) and 1(f)]. For example, the FB power spectrum of the first band RPS is located only within the first Brillouin zone [Fig. 1(e)].

In conclusion, we have presented random phase solitons in nonlinear periodic lattices. For RPSs to exist, their intensity profiles, power spectra, and coherence properties must conform to the lattice periodicity. We find equivalent conclusions to hold in lattices with Kerr nonlinearity, and in optically induced arrays with saturable nonlinearity [9–11]. Finally, we emphasize that the dynamics of partially coherent waves in nonlinear periodic lattices is a general problem, occurring in contexts besides spatial beams in waveguide arrays, e.g., partially coherent temporal pulses in nonlinear photonic crystals, or weakly correlated BEC systems in periodic traps, etc.

This work was supported by the MURI program on solitons, by the German-Israeli DIP project, by the Israel–USA Binational Science Foundation, and by the Ministry of Science, Israel.

[1] A. S. Davydov, J. Theor. Biol. **38**, 559 (1973).
[2] W. P. Su, J. R. Schieffer, and A. J. Heeger, Phys. Rev. Lett. **42**, 1698 (1979).
[3] D. N. Christodoulides and R. I. Joseph, Opt. Lett. **13**, 794 (1988).
[4] P. Binder *et al.*, Phys. Rev. Lett. **84**, 745 (2000).
[5] A. Trombettoni and A. Smerzi, Phys. Rev. Lett. **86**, 2353 (2001).
[6] H. Eisenberg *et al.*, Phys. Rev. Lett. **81**, 3383 (1998).
[7] H. Eisenberg *et al.*, Phys. Rev. Lett. **85**, 1863 (2000); T. Pertsch *et al.*, Phys. Rev. Lett. **88**, 093901 (2002); M. J. Ablowitz and Z. H. Musslimani, Phys. Rev. Lett. **87**, 254102 (2001).
[8] R. Morandotti *et al.*, Phys. Rev. Lett. **83**, 2726 (1999); T. Pertsch *et al.*, Phys. Rev. Lett. **83**, 4752 (1999).
[9] N. K. Efremidis *et al.*, Phys. Rev. E **66**, 046602 (2002).
[10] J.W. Fleischer *et al.*, Phys. Rev. Lett. **90**, 023902 (2003).
[11] J.W. Fleischer, M. Segev, N. K. Efremidis, and D. N. Christodoulides, Nature (London) **422**, 147 (2003).
[12] D. Mandelik *et al.*, Phys. Rev. Lett. **90**, 053902 (2003).
[13] O. Cohen *et al.*, Phys. Rev. Lett. **91**, 113901 (2003); A. A. Sukhorukov and Y. S. Kivshar, Phys. Rev. Lett. **91**, 113902 (2003).
[14] D. N. Christodoulides, F. Lederer, and Y. Silberberg, Nature (London) **424**, 817 (2003).
[15] M. Mitchell, Z. Chen, M. Shih, and M. Segev, Phys. Rev. Lett. **77**, 490 (1996); M. Mitchell and M. Segev, Nature (London) **387**, 880 (1997).
[16] D. N. Christodoulides, T. H. Coskun, M. Mitchell, and M. Segev, Phys. Rev. Lett. **78**, 646 (1997).
[17] M. Mitchell, M. Segev, T. H. Coskun, and D. N. Christodoulides, Phys. Rev. Lett. **79**, 4990 (1997).
[18] V.V. Shkunov and D. Anderson, Phys. Rev. Lett. **81**, 2683 (1998).
[19] M. Soljacic *et al.*, Phys. Rev. Lett. **84**, 467 (2000); D. Kip *et al.*, Science **290**, 495 (2000).
[20] H. Buljan *et al.*, Opt. Lett. **28**, 1239 (2003).
[21] D. N. Christodoulides *et al.*, Phys. Rev. E **63**, 035601 (2001).